frontiers in Immunology

TYPE Original Research
PUBLISHED 15 May 2026
DOI 10.3389/fimmu.2026.1847411

OPEN ACCESS

EDITED BY
Irina Tcherepanova,
Consultant, Chapel Hill, United States

REVIEWED BY
Zongde Zhang,
Southwest Medical University, China
Rajesh Kumar,
Seattle Children's Hospital, United States

*CORRESPONDENCE
Eric Tran
Eric.Tran@providence.org

RECEIVED 04 April 2026
REVISED 23 April 2026
ACCEPTED 27 April 2026
PUBLISHED 15 May 2026

CITATION
Shih Y-P, Drokin S, Burke O, Huang H, Leung A, Bravo-Manriquez M, Jang M, Syrkina MS, Julian L, Sanjuan N and Tran E (2026) Clinical-scale 10-day TCR-T cell manufacturing using IL-2/7/15 and TGF-β promotes early memory and tissue-resident-like phenotypes and robust antitumor activity *in vitro*. *Front. Immunol.* 17:1847411. doi: 10.3389/fimmu.2026.1847411

Clinical-scale 10-day TCR-T cell manufacturing using IL-2/7/15 and TGF-β promotes early memory and tissue-resident-like phenotypes and robust antitumor activity *in vitro*

Yi-Ping Shih, Stephan Drokin, Olivia Burke, Huayu Huang, Amy Leung, Marco Bravo-Manriquez, Myungkyu Jang, Marina S. Syrkina, Laura Julian, Nelson Sanjuan and Eric Tran*

Earle A. Chiles Research Institute, a division of Providence Cancer Institute, Portland, OR, United States

Background: Adoptive cell therapy (ACT) using TCR-engineered T (TCR-T) cells is a promising strategy for treating solid tumors. One factor that influences the efficacy of ACT is the type of T cells used, with T cells displaying younger, less differentiated or tissue resident phenotypes associated with greater antitumor activity. We aimed to develop a rapid, clinical-scale protocol to generate younger and more potent TCR-T cells for therapy.

Methods: Patient-derived PBMC were stimulated, CD8+ enriched, retrovirally transduced to express KRAS G12D-targeting TCRs, and expanded for 10 days in the presence of a novel cytokine cocktail (CKT) containing IL-2, IL-7, IL-15, and TGF-β. The impact of CKT on the phenotype, effector function, and *in vitro* antitumor activity was evaluated and compared to TCR-T cells manufactured with IL-2. This process was then adapted for clinical-scale manufacturing.

Results: TCR-T cells generated with CKT displayed an increased frequency of early memory (Tn/scm) and tissue-resident (Trm)-like T cells with decreased KLRG1 expression compared to IL-2 manufactured TCR-T cells. CKT manufactured TCR-T cells demonstrated higher 4-1BB upregulation, IFN-γ, TNF, and granzyme B (GZMB) production, and enhanced killing of pancreatic and colorectal cancer cell lines in 2D and 3D tumor spheroid co-culture. Clinical-scale engineering runs yielded 3.30 and 6.15 x 10^9 total cells that displayed similar phenotypic and functional attributes observed in the small-scale studies.

Conclusion: Our novel 10-day TCR-T manufacturing protocol using IL-2, IL-7, IL-15, and TGF-β generates TCR-T cells characterized by distinct memory and tissue residency markers such as CCR7, CD103, and CD49a, and potent effector functions with the potential to improve the efficacy of adoptive cell therapy.

KEYWORDS
adoptive cell therapy, central memory T cells, KRAS, solid cancers, stem-like T cells, TCR-gene therapy, tissue resident memory T cells

Introduction

T-cell receptor-engineered T-cell (TCR-T) therapy is a type of adoptive cell therapy where a patient's autologous peripheral blood T cells are genetically engineered to express a TCR that targets an antigen expressed by the patient's tumor. Promising clinical activity in solid tumors has been observed with TCR-T therapy targeting tumor antigens such as NY-ESO-1 (1–7), MAGE-A3 (8, 9), MAGE-A4 (10, 11), PRAME (12), HPV16-E6 (13) and E7 (14), TP53 R175H (15), KRAS G12D (16), as well as personalized mutations (17). Approximately 40% of patients with synovial sarcoma experienced a clinical response after TCR-T therapy targeting MAGE-A4 (10), leading to the FDA approval of the first TCR-T therapy (afamitresgene autoleucel) in 2024 for this indication. However, despite promising clinical activity, there currently are no published reports of durable complete responses mediated by TCR-T therapy in patients with metastatic solid cancers outside of melanoma. Thus, there is an urgent need to improve the efficacy of TCR-T therapy for metastatic epithelial cancers.

Different T-cell subsets have different capacities to eliminate tumors. A wealth of data in mouse tumor models have demonstrated that the adoptive transfer of less differentiated CD8+ T cells such as stem cell memory (Tscm) and central memory (Tcm) T cells is more effective at mediating tumor regression than effector (Teff) and terminally differentiated effector (Tte) T cells (reviewed in (18)). Correlative data in human adoptive tumor-infiltrating lymphocyte (TIL) therapy (19) and chimeric antigen-receptor (CAR) T-cell therapy (20–24) also have implicated a role for less differentiated T cells in mediating antitumor responses. In addition to Tscm and Tcm, other T-cell subsets may be desirable for use in adoptive cell therapy (ACT). For example, tissue resident memory T cells (Trm) are associated with favorable outcomes and clinical responses to immunotherapy in a variety of human cancers (reviewed in (25) and (26)). While there are limited studies on the use of Trm for ACT, the transfer of Trm-like CAR-T cells was superior to conventional CAR-T cells in solid and liquid tumor xenograft models (27), and the transfer of T cells resembling Trm through deletion of *Vhl* or overexpression of the Runx3 transcription factor led to improved control of syngeneic mouse tumors (28, 29). Clinically, we previously reported a patient with metastatic pancreatic ductal adenocarcinoma (PDAC) who achieved a clinical response following the infusion of KRAS G12D-targeted TCR-T cells; these cells were skewed toward a Trm-like phenotype by manufacturing in the presence of TGF-β (16).

A unique feature of ACT is the ability to manipulate cell culture conditions to generate T cells with desired phenotypes and functional attributes. Indeed, cytokines such as IL-7, IL-15, and IL-21 can promote the generation of human Tscm and/or Tcm (30–34) while TGF-β has been used to generate human Trm-like T cells (16, 27). Here, we developed a 10-day TCR-T cell manufacture protocol that uses the novel cytokine combination of IL-2, IL-7, IL-15, and TGF-β and G-Rex bioreactors. We found that TCR-T products manufactured with this cytokine cocktail (CKT) were enriched in Tscm, Tcm, and Trm-like cells compared to cells manufactured with IL-2 alone. Moreover, CKT manufactured TCR-T cells exhibited superior cytotoxic ability and effector cytokine production against tumor cell lines than those grown with IL-2 alone. Engineering runs in our cleanroom facility using patient peripheral blood mononuclear cells (PBMCs) produced 3.3–6.1 × 10^9 CD8-enriched cells with an average TCR transduction efficiency of 85%. Thus, this new manufacturing process can generate clinically relevant numbers of TCR-T cells with desirable attributes for ACT.

Materials and methods

Patient samples

Leukapheresis products were obtained from patients through an IRB-approved tissue procurement protocol (IRB number 2018000418). PBMCs were isolated from leukapheresis products using standard Ficoll-Paque density gradient methods and PBMCs were cryopreserved in CryoStor10 (BioLife Solutions). PBMCs used in this study were derived from two patients with colorectal cancer (CRC), CRI-5268 and CRI-5126 (both HLA-C*08:02 genotype), and two patients with pancreatic ductal adenocarcinoma (PDAC), CRI-5178 and CRI-2890 (HLA-A*11:01 and HLA-C*08:02 HLA genotype, respectively).

Cell lines

The endogenous KRAS G12D-positive cell lines including the pancreatic adenocarcinoma cell lines HPAC and HPAFII as well as the colorectal adenocarcinoma cell lines LS513 and LS180 were acquired from the American Type Culture Collection (ATCC). These cell lines were retrovirally transduced to stably express HLA-C*08:02 and green fluorescent protein (GFP), or HLA-A*11:01 and GFP, with the HLA and GFP genes separated by a 2A self-cleaving peptide sequence. All cell lines were cultured in Dulbecco's Modified Eagle Medium (DMEM, Gibco) supplemented with high glucose, GlutaMax, 10% fetal bovine serum (FBS, Gibco), and 1% penicillin/streptomycin.

TCRs and retroviral vectors

The three KRAS G12D-reactive TCRs used in this study have been previously characterized (16, 35, 36). Two HLA-C*08:02-restricted TCRs were used: the C08-9mer TCR which recognizes the 9mer GA**D**GVGKSA peptide, and the C08-10mer TCR which recognizes the 10mer GA**D**GVGKSAL peptide. The third TCR, A11-10mer TCR, is HLA-A*11:01 restricted and recognizes the 10mer VVVGA**D**GVGK peptide. Each TCR contains the mouse TCRα and TCRβ constant regions, which promotes pairing of the introduced TCR and allows for the identification of the TCR-transduced T cells using an anti-mouse TCRβ constant region antibody. Gammaretroviral vector for each TCR was produced under GMP by the Vector Production Facility at Cincinnati Children's Hospital Medical Center. Retroviral vectors (RV) passed safety tests including cell-based assays for adventitious viruses and replication competent retrovirus, as well as mycoplasma, sterility, and endotoxin. Adventitious virus and replication competent retrovirus testing on the RV was performed by the

National Gene Vector Biorepository at Indiana University which is funded through the National Heart Lung and Blood Institute contract 75N92019D00018.

TCR-T cell transduction and expansion, small-scale

PBMC were thawed and 48×10^6 cells were stimulated with 50 ng/mL anti-CD3 (clone OKT3, Miltenyi Biotec) in TCR-CKT2–5 complete medium which comprised AIM-V CTS media (Gibco), 5% human AB serum (GeminiBio) with the appropriate cytokines 300 IU/mL IL-2 (R&D Systems, GMP-grade), 30 ng/mL IL-7 (R&D Systems, GMP-grade), 20 ng/mL IL-15 (R&D Systems, GMP-grade), and 5 ng/mL TGF-β (Biolegend, GMP-grade). PBMC were seeded in one T-75 flask (48 mL/flask, 1×10^6/mL) and incubated at 37 °C, 5% CO_2 for two days. Non-treated tissue culture 6-well plate was coated with 10 μg/mL RetroNectin (2 mL/well, Takara Bio) a day prior to transduction and stored overnight at 4 °C. After two days, stimulated cells were harvested and $CD8^+$ T cells were enriched by $CD4^+$ depletion using CliniMACS CD4 MicroBeads at 3 times the recommended bead amount and LS columns (Miltenyi Biotec). RetroNectin plates were loaded with 4 mL retroviral vector (optimized dilution to achieve <5 VCN/cell) and centrifuged at $2000 \times g$, 32 °C for 2 h. Retroviral supernatant were then aspirated and 2×10^6 $CD8^+$ T cells were added per transduced well (4 mL/well). Plates were centrifuged at $400 \times g$ for 10 min and incubated overnight at 37 °C, 5% CO_2. After one day, transduced cells from one well were transferred into a well of a G-Rex 6M-2 plate (Wilson Wolf) and filled to 20 mL using TCR-CKT2–5 media. On day 7, 16 mL of media was removed from each well, and replenished with fresh TCR-CKT2–5 media. Transduced T cells were harvested on day 10 for experiments, quality control assays, and remaining cells were cryopreserved using CryoStor10 (BioLife Solutions).

TCR-T cell transduction and expansion, clinical-scale

Manufacturing was performed in our GMP-capable cleanroom facility. PBMCs were thawed and 1.2×10^9 cells were stimulated using the same GMP-grade reagents as the small-scale process and seeded in six T-300 flasks (192 mL/flask, 1×10^6/mL) and incubated at 37 °C, 5% CO_2 for two days. Non-treated tissue culture 6-well plates were coated with 10 μg/mL RetroNectin (2 mL/well, Takara Bio, GMP-grade) a day prior to transduction and stored overnight at 4 °C. For one TCR, 12 plates (72 wells) were prepared; for two TCRs, 6 plates per TCR (36 wells each). After two days, stimulated cells were pooled and $CD8^+$ T cells were enriched by $CD4^+$ depletion using CliniMACS CD4 MicroBeads at 3 times the recommended bead amount and LS columns (Miltenyi Biotec). RetroNectin plates were loaded with 4 mL retroviral vector (optimized dilution to achieve <5 VCN/cell) and centrifuged at $2000 \times g$, 32 °C for 2 h. Retroviral supernatants then were aspirated and 2×10^6 $CD8^+$ T cells were added per retronectin-coated well (4 mL/well, 144×10^6 $CD8^+$ cells total). Plates were centrifuged at $400 \times g$ for 10 min and incubated overnight at 37 °C, 5% CO_2. After one day, transduced T cells were transferred into a G-Rex 100M flask (Wilson Wolf) (34 or 35 wells per flask) and filled to 1000 mL using TCR-CKT2–5 media. On day 7, 600 mL of media was removed from each flask and fresh TCR-CKT2–5 media was added to the flasks. Transduced T cells were harvested on day 10 via the LOVO system (Fresenius Kabi) and formulated into the drug product with 250 mL buffer consisting of Plasmalyte (Baxter) + 2% human serum albumin (GRIFOLS). The drug products underwent experiments, quality control assays, and aliquots of cells were cryopreserved using CryoStor10 (BioLife Solutions). Key quality control assays included transduction efficiency (mTCRβ) by flow cytometry, MSGV1 vector copy number (VCN) by QPCR, in-process testing for replication-competent retrovirus (RCR) by QPCR for the envelope RD114, sterility testing using the BacT/Alert system (bioMérieux) with iLYM, iNST, and iAST culture bottles to detect a broad range of bacteria, yeasts, and molds, mycoplasma testing using the MycoTOOL RT-PCR kit (Roche), and endotoxin detection with EndoSafe nexgen-PTS (Charles River).

Flow cytometry staining

For T-cell phenotyping studies, unless otherwise indicated, cells were thawed and rested overnight in media containing the cytokines that were used to manufacture the TCR-T cells. The next day, cells were harvested and stained at 10 μL/well in a 96-well U-bottom plate with a pre-titrated antibody panel prepared in FACS buffer (PBS with 2% FBS, 2 mM EDTA). Cells were stained for 30 min at 4 °C in the dark, washed with FACS buffer, and then resuspended in 100 μL of FACS buffer containing propidium iodide for live/dead cell analysis. Samples were acquired with a Cytoflex LX cytometer and analyzed with FlowJo v10. The following antibodies were used (all from BioLegend, except the γδ TCR antibody which was from BD Biosciences): AF700-CD3 (SK7), BV510-CD8 (RPA-T8), PE/Cy7-CD45RO (UCHL1), BV421-CCR7 (G043H7), FITC or PE/Cy7-CD103 (Ber-ACT8), Alexa Fluor647-CD49a (TS2/7), APC-fire 750-CD69 (FN50), BV421- γδ TCR (11F2), APC-CD56 (5.1H11), PE-PD1 (EH12.2H7), PE-KLRG1 (SA231A2), APC-fire750-LAG3 (11C3C65), APC-fire 750 or PE-mTCRβ (H57-597), APC-4-1BB (4B4-1), APC-fire 750-CD4 (SK3).

Overnight co-culture assay to evaluate T-cell activation by flow cytometry

Tumor cell lines were harvested using 2.5% trypsin-EDTA (Life Technologies). Once the cells detached from the plates, DMEM media was added to quench the reaction. Tumor cells then were harvested, spun down and resuspended in the DMEM media. 10,000 tumor cells in 100 ul were seeded per well of a 96-well flat bottom plate and left to recover and adhere overnight. The following day, T cells were harvested, washed, and then resuspended in 50/50 media without exogenous cytokines. 50/50 media comprised 50% AIM-V (Gibco) with 50% RPMI 1640 medium (Cytiva) containing 10% human AB serum (Valley Biomedical), 25mM Hepes (Cytiva), 10 μg/ml Penicillin-Streptomycin solution (Cytiva), 2 mM GlutaMax (Gibco), and 5 μg/ml Gentamicin (Thermo Fisher Scientific). 50,000 T cells in

100 µL then were added per well for co-culture. After overnight incubation, supernatants and cells were harvested and each transferred to a new 96-well U-bottom plate. Cells underwent staining with antibodies targeting CD3, CD8, mTCRβ, CD103 and 4-1BB followed by flow cytometry analysis as described above.

Analysis of cytokines in supernatants

Co-culture assays were set up as described above with the following modifications: for coculturing with tumor cell lines, 50,000 tumor cells were plated either 4h or overnight before coculture with 100,000 T cells per well. For coculturing with peptide-pulsed antigen presenting cells (autologous PBMC), PBMC first were thawed, resuspended in 50/50 media at 4×10^6 cells/mL and rested overnight in an ultra-low attachment flask at 37 °C and 5 % CO_2. The following day, the PBMC were harvested, washed, and seeded at 2×10^6 cells/well (1 mL) in ultra-low attachment 24-well plates. The cells then were pulsed for 2–4 h at 37 °C with 1 µg/mL of either wild-type KRAS or mutant KRAS G12D peptides (HPLC-purified, from Genscript or Lifetein). The peptides used were GA**D**GVGKSA and GA**D**GVGKSAL for the HLA-C*08:02-restricted TCRs and VVVGA**D**GVGK for the HLA-A*11:01-restricted TCR. PBMC were then washed twice with PBS and resuspended in 50/50 media and 2×10^5 PBMC were cocultured with 1×10^5 T cells. After overnight coculture, 140 µL of supernatants were harvested from each well and frozen. Supernatants were thawed and the LEGENDplex™ Human CD8/NK Panel V02 (BioLegend) was used for multiplex cytokine quantification following the manufacturer's protocol except with the modification that all experimental sample and reagent volumes were each reduced to 15 µL per well. Supernatants were not diluted for the assay. Samples and standards were acquired on a Cytek Aurora flow cytometer. Data was analyzed using the LEGENDplex™ Data Analysis Software Suite (BioLegend).

In vitro cancer cell killing assay, 2D culture

Human cancer cell lines stably expressing HLA-C*08:02 and GFP were seeded into a 96-well flat bottom plate at a density of 1×10^4 cells per well in DMEM media. The following day, TCR-Td cells were added to tumor cells at the indicated effector to target (E:T) ratios and cocultured for 5 days in an incubator at 37 °C with 5% CO2. GFP signal was monitored using the Cellcyte live-cell analysis system (Cytena). Images were captured every 12 hours for up to 120 hours. GFP signal intensity in each well was quantified using Cellcyte software. A decrease in GFP signal represented tumor cell death and was correlated with morphological changes in the tumor cells consistent with cell death such as cell shrinkage, membrane blebbing, and loss of adhesion.

In vitro cancer cell killing assay, 3D spheroid culture

Tumor spheroids were generated using HPAC-C*08:02-GFP, HPAFII-C*08:02-GFP, LS513-A*11-GFP and LS180-A*11-GFP cell lines. For spheroid formation, 2,500–5,000 tumor cells per well were seeded into 96-well ultra-low attachment PrimeSurface plates (S-bio) in 100 µL of complete medium. Plates were centrifuged at 125 × g for 10 minutes at room temperature to facilitate cell aggregation. Spheroids were incubated at 37 °C with 5% CO_2 for 72 hours to allow for compact spheroid formation. On the day of the assay, 100 µL of T cells were added to achieve the desired E:T ratios. Spheroid size and fluorescence intensity were quantified using Cellcyte software.

Statistical methods

Paired t-tests were performed using GraphPad Prism version 10.6.1 (GraphPad Software, San Diego, CA, USA), with $p < 0.05$ considered statistically significant. Graphs display mean ± SEM for biological replicates, or mean ± SD for technical replicates.

Results

Manufacturing TCR-T cells with the cytokine cocktail IL-2, IL-7, IL-15, and TGF-β enriches for early memory (Tn/scm) and tissue-resident memory (Trm)-like phenotypes

Our previous TCR-T manufacturing process comprised of two *in vitro* stimulation steps that totaled nearly 4 weeks (16). Toward the goal of generating younger and more potent TCR-T cells for ACT, we shortened the manufacture time to 10 days, incorporated a CD8-enrichment step, and evaluated the use of IL-2, IL-7, IL-15, and TGF-β during cell culture (Figure 1A). The CD8-enrichment step was included to better standardize product composition across variable patient samples and promote optimal potency, given that HLA-I-restricted TCRs typically have higher functional avidity in CD8 T cells than in CD4 T cells. PBMC from three patients, two with colorectal cancer (CRC; CRI-5268 and CRI-5126) and one with pancreatic ductal adenocarcinoma (PDAC; CRI-5178) were thawed and stimulated with anti-CD3 (OKT3) in the presence of either IL-2 or the cytokine cocktail (CKT) IL-2, IL-7, IL-15, and TGF-β. Two days later, CD8 cells were enriched by removing CD4 cells using magnetic beads followed by genetic insertion of KRAS G12D-reactive TCRs with gammaretroviral vectors. CRI-5268 and CRI-5126 T cells were engineered to express two different HLA-C*08:02-restricted TCRs (each TCR in a separate aliquot), while CRI-5178 T cells were engineered to express an HLA-A*11:01 restricted TCR, resulting in five different samples for evaluation (Figure 1B). Cells were expanded for a total of 10 days prior to evaluation. As seen in Figures 2A–C, cell expansion and TCR transduction efficiency were comparable between the IL-2 and CKT conditions despite the presence of TGF-β in CKT. T cells comprised the majority (> 90%) of total cells (Figure 2D), and within this T-cell population, most were CD8+ T cells while γδ T cells accounted for less than 1% in both IL-2 and CKT manufacture groups (Figure 2E). CD56+ NK cells dominated the CD3-negative cell compartment (Figure 2F). Collectively, these results demonstrate efficient enrichment of CD8+ T cells from patient PBMCs that initially contained 65 to 80% CD4+ T cells (Supplementary

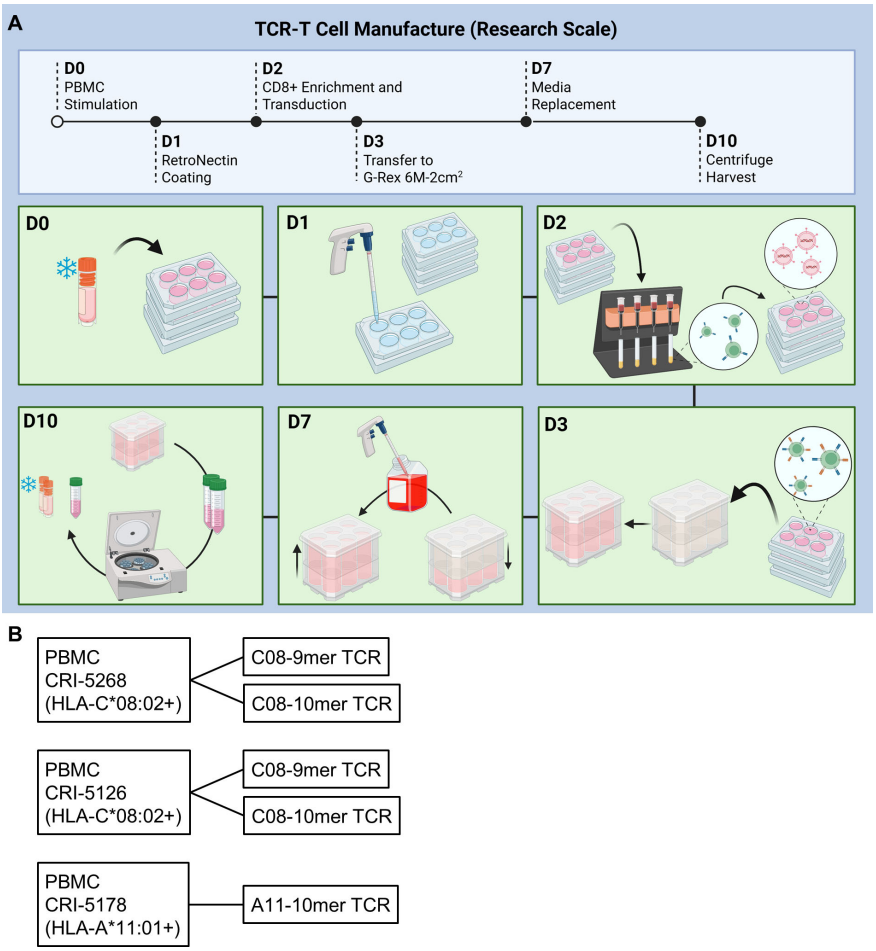

FIGURE 1
10-day TCR-T manufacture process. **(A)** Schematic and **(B)** samples evaluated and TCRs used in the small research-scale studies. Each sample was manufactured with either IL-2 or the cytokine cocktail (CKT) IL-2, IL-7, IL-15, and TGF-β. **(A)** was generated with BioRender.

Figure 1). Notably, TCR-T cells generated with CKT were enriched in naïve or stem cell memory (Tn/scm, CD45RO-CCR7+) and central memory (Tcm, CD45RO+CCR7+) as well as tissue resident memory-like (Trm, CD103, CD49a, and CD69) T cells compared to TCR-T generated with IL-2 (Figures 2G, H). The terminal differentiation marker KLRG1 and activation/exhaustion marker PD-1 were decreased while LAG3 was increased on CKT TCR-T cells compared to IL-2 TCR-T cells (Figure 2I). Representative flow cytometry plots are shown in Supplementary Figure 2.

TCR-T cells manufactured with IL-2, IL-7, IL-15, and TGF-β display robust effector function and antitumor activity *in vitro*

To evaluate the *in vitro* antitumor function of the TCR-T cells, we first measured expression of the T-cell activation marker 4-1BB after coculture with cancer cell lines expressing endogenous KRAS G12D that were transduced to express either HLA-C*08:02 or HLA-A*11:01. Across all three KRAS G12D TCRs and three patient donor T cells, CKT manufactured TCR-T displayed increased 4-1BB expression compared to IL-2 manufactured TCR-T cells (Figures 3A–C). While both IL-2 and CKT manufactured TCR-T cells could specifically produce relatively high levels of effector molecules upon stimulation with mutated KRAS peptides, CKT manufactured TCR-T cells secreted higher levels of IFN-γ (Figures 3D–F), TNF (Figures 3G–I), and granzyme B (Figures 3J–L) after coculture with multiple tumor cell lines compared to IL-2 manufactured TCR-T cells. This was associated with enhanced *in vitro* killing of different KRAS G12D+ GFP-expressing tumor cell lines expressing the appropriate HLA restriction element across different effector to target ratios in both 2D and 3D spheroid cultures by CKT versus IL-2 manufactured TCR-T cells as determined by quantification of GFP-positive tumor cells after coculture (see Figures 4A–E for 9mer-C08 TCR-T cells and Figures 4F–J for 10mer-C08 TCR-T cells from patient CRI-5268, and Supplementary Figures 3A–E for 9mer-C08 TCR-T cells and Supplementary Figures 3F–J for 10mer-C08 TCR-T cells from patient CRI-5126, and Supplementary Figures 3K–N for 10mer-A11 TCR-T cells from patient CRI-5178). CKT manufactured TCR-T cells generally demonstrated more rapid killing of 2D and 3D cancer cell lines compared to IL-2 manufactured TCR-T cells (Figures 4K–O).

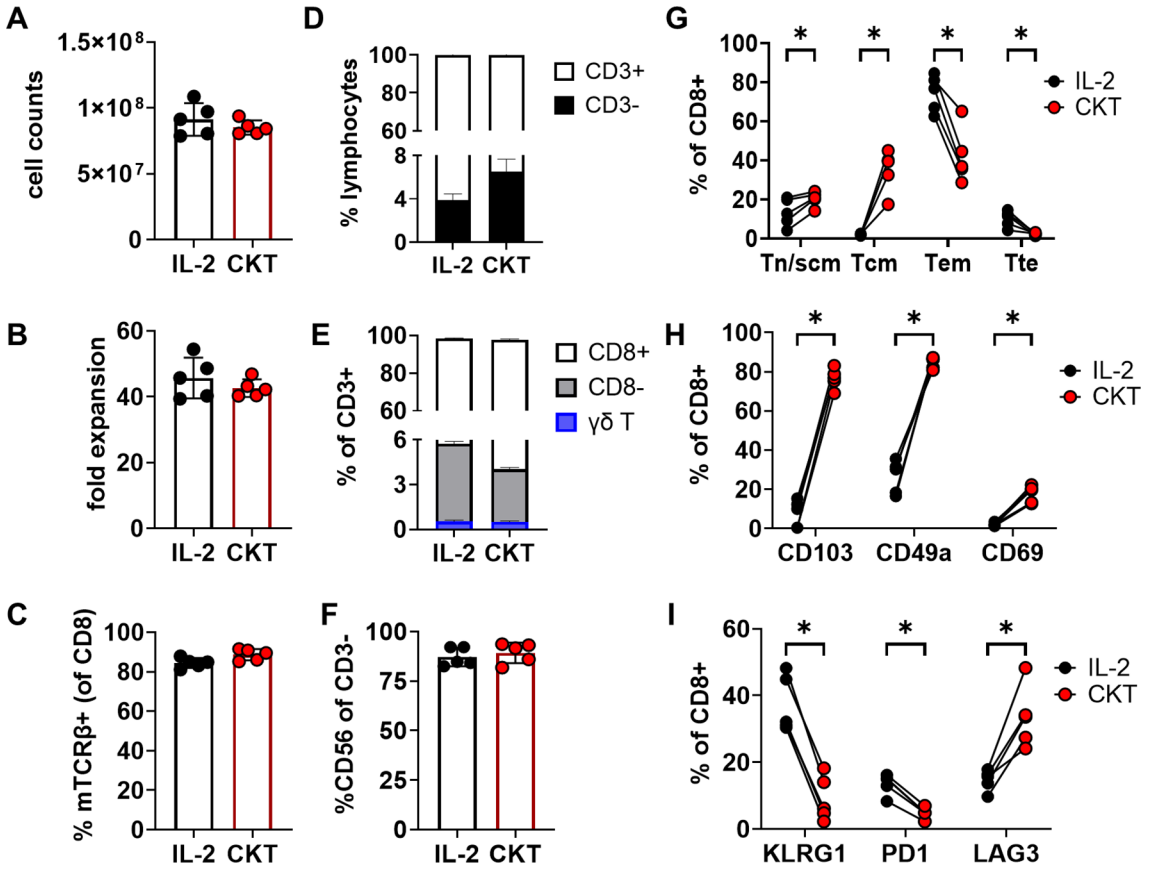

FIGURE 2
Cell number and phenotype of TCR-T cells after manufacture with IL-2 or cytokine cocktail (CKT) for 10 days. **(A)** Cell number, **(B)** fold expansion (from day 2 onwards), **(C)** transduction efficiency as determined by flow cytometric analysis of the mouse TCRβ constant region which is engineered into the TCRs. **(D)** Percent CD3+/- cells of live lymphocytes. **(E)** Frequencies of CD8+/- and γδ T cells. **(F)** Percent CD56+ cells of live CD3- cells. **(G)** T-cell differentiation, **(H)** tissue resident (Trm) and **(I)** exhaustion/activation markers were evaluated by flow cytometric analysis. Tn/scm: CD45RO-CCR7+; Tcm: CD45RO+CCR7+; Tem: CD45RO+CCR7-; Tte: CD45RO-CCR7-. Data from the three patient PBMCs and five TCR-T products are shown. *p < 0.05 by paired t-test.

Establishment of a clinical-scale TCR-T manufacturing process using the cytokine cocktail IL-2, IL-7, IL-15, and TGF-β

The favorable phenotype and robust antitumor activity observed with TCR-T cells produced in 10 days with CKT led us to develop a clinical-scale manufacturing protocol. This protocol (Figure 5A) was identical to our small-scale protocol (Figure 1A) except that reagents and materials were scaled up accordingly and the final infusion products were harvested with the LOVO Cell Processing System. To achieve clinically relevant TCR-T cell numbers, we stimulated 1.2 × 10^9 PMBC and transduced about 1.44 x 10^8 CD8-enriched T cells which were expanded in two G-Rex 100M flasks. We performed two engineering runs using PBMCs from patients with pancreatic cancer: CRI-5178, previously used in our small-scale studies, and CRI-2890, a new donor (Figure 5B). As seen in Figure 6A, the two CKT engineering runs with CRI-5178 and CRI-2890 yielded 3.30 and 6.15 x 10^9 total cells after harvest, about 98% and 85% CD8 T cells, and 86% and 85% TCR transduction efficiency, respectively. Consistent with the small-scale studies, the infusion products were composed predominantly of Tn/scm and Tcm (Figures 6B, C), with expression of the Trm markers CD103, CD69, and CD49a (Figures 6D, E), and variable expression of KLRG1, PD-1, and LAG3 (Figures 6F, G). Moreover, stimulation with mutated KRAS peptides or coculture with KRAS G12D+ tumor cell lines expressing the appropriate HLA led to robust production of IFN-γ, TNF, and GZMB (Figures 7A–F) which was associated with *in vitro* tumor cell line killing as expected (Figures 7G–J). Both CKT infusion products from the engineering runs passed safety tests including vector copy number (VCN), replication competent retrovirus (RCR), endotoxin, mycoplasma, and sterility (Supplementary Table 1).

Discussion

A major feature of ACT is the ability to manipulate manufacture conditions to endow T cells with desired phenotypic and functional attributes. Here, we developed a clinical-scale, 10-day manufacturing protocol utilizing a novel cytokine cocktail (CKT) containing IL-2, IL-7, IL-15, and TGF-β to generate TCR-T-cell products enriched in early memory and tissue-resident-like phenotypes and with enhanced *in vitro* effector function and antitumor

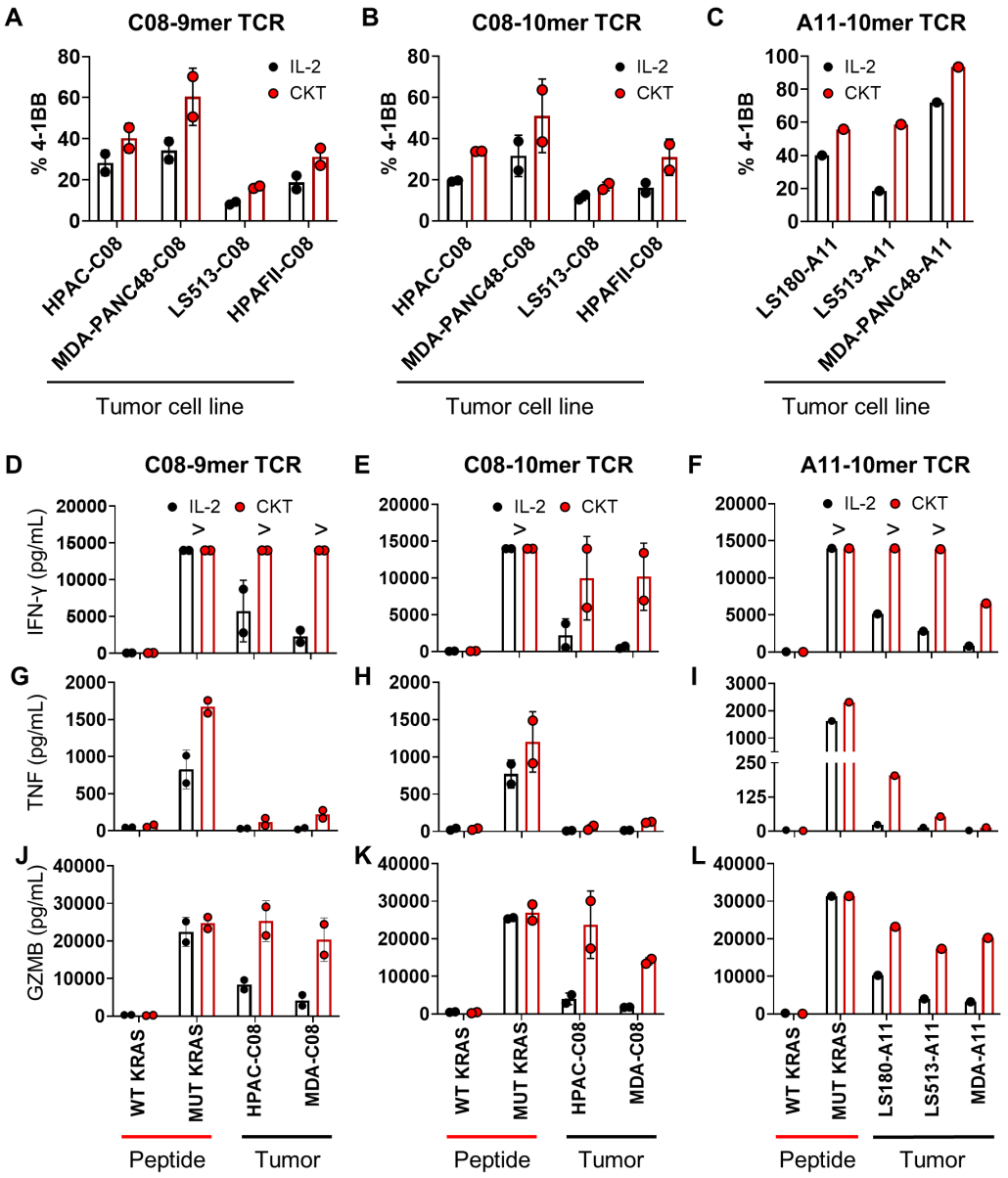

FIGURE 3
Tumor cell line reactivity and effector function of KRAS G12D-reactive TCR-T cells manufactured with either IL-2 or CKT. IL-2 (black) or CKT (red) manufactured TCR-T cells were cocultured overnight with the indicated KRAS G12D+ tumor cell lines expressing either HLA-C*08:02 (C08) or HLA-A*11:01 (A11), or autologous PBMC pulsed with 1 μg/mL of wild-type (WT) or mutated (MUT) KRAS peptide and **(A–C)** 4-1BB expression was measured by flow cytometry and **(D–F)** IFNγ, **(G–I)** TNF, and **(J–L)** granzyme B (GZMB) was measured in the supernatants using the LegendPlex assay. For the C08-9mer TCR and C08-10mer TCR, the two HLA-C*08:02+ patient samples (CRI-5126 and CRI-5268) were pooled. Flow cytometry data were gated on CD3+CD8+mTCRβ+ T cells. ">" greater than assay detection limit. Coculture assays are representative of at least 2 independent experiments. LEGENDplex data were from one experiment with technical replicates.

ability. A large body of evidence exists demonstrating the superiority of early memory T cells over more differentiated T cells in antitumor immunity (18) and thus we utilized IL-7 and IL-15 for their established roles in promoting T-cell proliferation while preserving Tn/scm and Tcm phenotypes during cell manufacture (30, 32, 33). Although IL-2 is a known driver of terminal differentiation (37, 38), it was included in our cytokine cocktail because preclinical observations in one of our patient-derived PBMC samples indicated that IL-7 and IL-15 alone were insufficient to drive robust TCR-T cell expansion; the addition of IL-2 rescued this proliferative capacity (data not shown). Notably, despite the inclusion of IL-2, a significant fraction of early memory T cells was preserved in the final TCR-T cell products across all four patient samples (Figures 2G, 6B, C). The final component of our CKT is TGF-β which is perhaps most well known as an immunosuppressive cytokine but has pleiotropic effects that are context dependent (39). Indeed, we incorporated TGF-β because of its critical role in generating Trm (40–44), which are positively correlated with patient survival in many tumor types as well as implicated in mediating responses to immunotherapy (25, 26).

The exact mechanisms of how our CKT-manufactured TCR-T cells mediate improved antitumor activity have not been fully elucidated but this and prior studies may provide some insight. In the setting of preclinical ACT studies, the use of TGF-β to generate

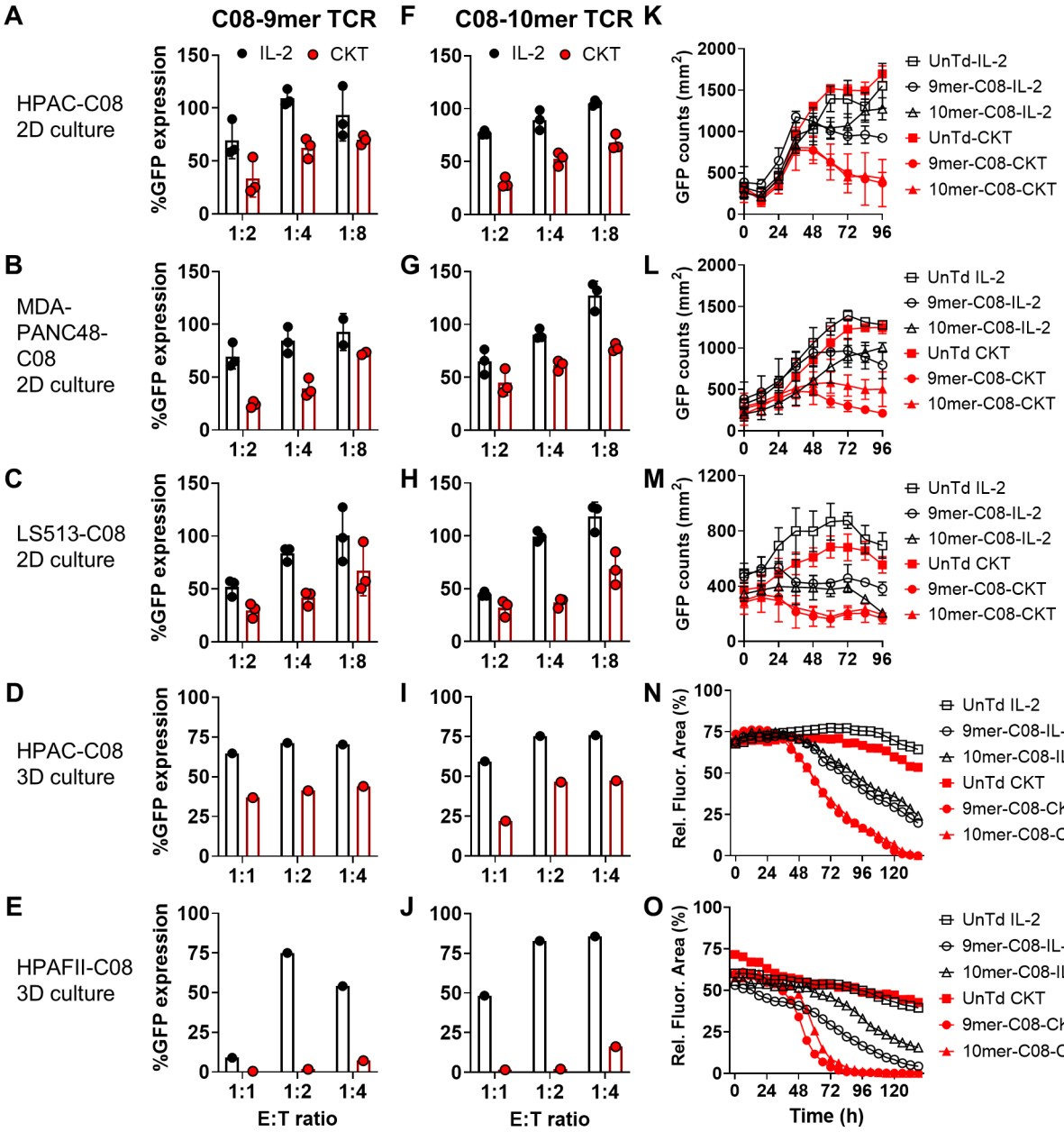

FIGURE 4
Tumor cell killing by IL-2 or CKT manufactured TCR-T cells from patient CRI-5268 in 2D and 3D coculture. **(A–E)** 9mer-C08 TCR-T cells manufactured with IL-2 (black) or CKT (red) were cocultured with the indicated KRAS G12D+ and HLA-C*08:02+ GFP-expressing tumor cell lines at various effector to target (E:T) ratios in **(A–C)** 2D or **(D, E)** 3D spheroid culture and GFP was quantitated at 72 h. **(F–J)** Same as **(A–E)** except with 10mer-C08 TCR-T cells. 100% GFP expression indicates the % GFP+ tumor cells in coculture wells containing control untransduced T cells manufactured with IL-2 or CKT. **(K–O)** IL-2 (black) or CKT (red) manufactured untransduced (UnTd), 9mer-C08, or 10mer-C08 TCR-T cells were cocultured with the same KRAS G12D+ and HLA-C*08:02+ GFP-expressing tumor cell lines described above at 1:2 E:T ratio in **(K–M)** 2D culture, or 1:4 E:T ratio in **(N, O)** 3D spheroid culture and GFP was quantitated over time using the Cellcyte live cell imager. Rel. Fluor. Area: relative fluorescence area. All data are representative of at least 2 independent experiments.

more effective human T cells was first reported in the setting of tumor-infiltrating lymphocytes (TIL) (45). In this study, addition of TGF-β at the beginning of the rapid expansion protocol favored growth of CD8 TIL over CD4 TIL which led to enrichment of melanoma antigen (MART1)-reactive CD8+ TIL and increased antitumor activity *in vitro*. In another study (46), TGF-β exposure during cell manufacture programmed T cells into a Tcm state with high polyfunctionality and proliferative potential which was associated with improved control of tumor xenografts by BCMA-targeted CAR-T cells. More recently, Jung et al. incorporated TGF-β during CAR-T cell manufacture which drove chromatin and transcriptional changes that promoted both stem-like and Trm phenotypes leading to improved tumor clearance via increased effector cytokine production, tumor infiltration, and *in vivo* persistence (27). Our CKT manufactured TCR-T cells similarly demonstrated an increase in early memory/Trm phenotypes and effector cytokine production. However, unlike Jung et al. who observed a decrease in cytotoxicity *in vitro* when TGF-β was added to IL-2

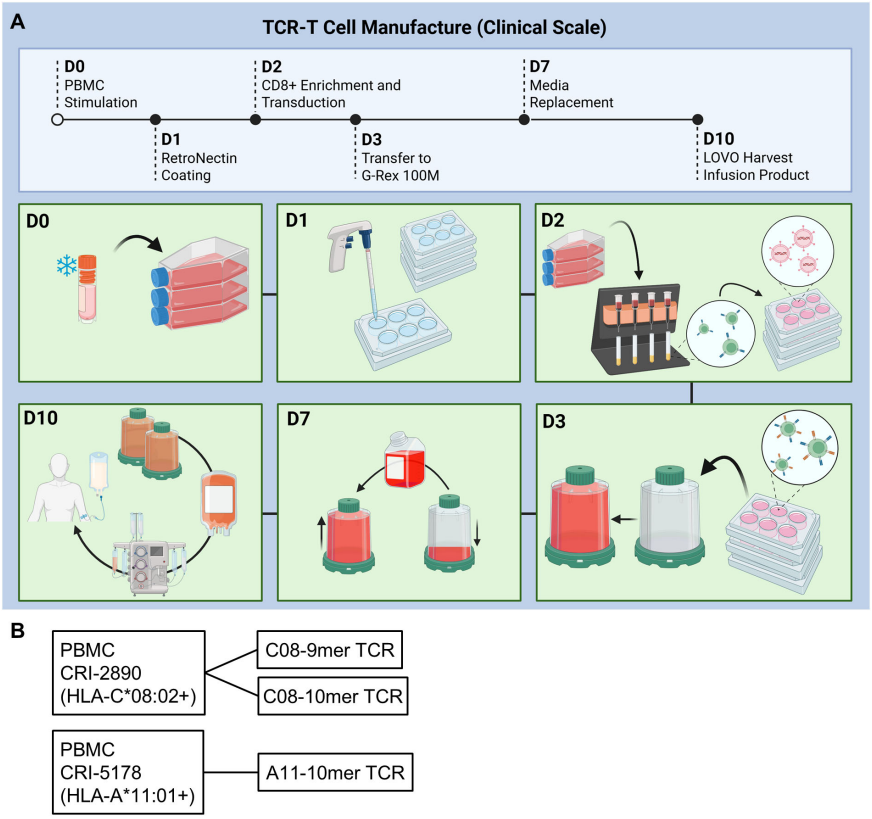

FIGURE 5
Clinical scale 10-day TCR-T manufacture process using CKT. **(A)** Schematic and **(B)** samples evaluated and TCRs used in the clinical-scale engineering runs. **(A)** was generated with BioRender.

during CAR-T cell manufacture, we found that CKT increased granzyme B production and cytotoxicity relative to IL-2 manufactured TCR-T (Figures 3K, J, L; Figure 4; Supplementary Figure 3). Furthermore, while Jung et al. observed decreased *KLF2* gene expression, which is consistent with a Trm phenotype, we did not observe this trend at the protein level in CKT-manufactured TCR-T cells (data not shown). This could be a consequence of CKT containing IL-7 and IL-15 which are known to promote expression of KLF2 (47, 48). Beyond cytokine signaling, these discrepancies also could be influenced by our use of patient-derived PBMCs and specific enrichment for CD8+ T cells, which may create a distinct epigenetic and metabolic starting point compared to the healthy donor PBMCs and mixed CD4/CD8 products used by Jung et al. Additional transcriptomic, epigenetic, and proteomic studies on CKT and IL-2 manufactured TCR-T cells would shed further light into the mechanisms responsible for these improved antitumor attributes. Notably, the effects of TGF-β on enhancing T-cell function do not appear restricted to conventional αβ T cells since γδ (Vγ9Vδ2) T cells expanded with IL-2 and TGF-β also demonstrate enhanced effector cytokine production, cytotoxicity, and antitumor activity compared to those expanded with IL-2 (49, 50).

While our current study demonstrated that TCR-T cells generated in 10 days with CKT displayed improved phenotype and function compared to those produced with IL-2, we further evaluated these cells against our previous manufacturing standard. This original protocol was a two-phase process involving initial PBMC stimulation and transduction, followed by a rapid expansion protocol (REP) to generate the final infusion product as described in Leidner et al. (16). Notably, we had previously manufactured a clinical-scale infusion product for patient CRI-2890 using this IL-2 based two-step method (V1; Supplementary Figure 4A), which allowed for a direct comparison between the two manufacturing approaches. In contrast to the CRI-2890 CKT infusion product (Figures 6C, E, G), the V1 product consisted almost entirely of Tem and Tte cells that lacked CD103 and CD69 expression and showed elevated KLRG1, though they maintained lower levels of PD-1 and LAG3 (Supplementary Figures 4B–D). Furthermore, we observed increased tumor cell killing by the CKT manufactured infusion product compared to the V1 infusion product of patient CRI-2890 (Supplementary Figures 4E, F). Taken together, these data indicate that TCR-T cells generated using CKT exhibit a more favorable phenotypic and functional profile than those produced by two distinct IL-2-based protocols.

Most TCR-T cell products evaluated in clinical trials to date employ HLA-I-restricted TCRs and are generated from bulk PBMCs without subset enrichment (1–7, 9–16, 51). Although this approach simplifies manufacturing, the resulting variability in CD4+ and CD8+ T-cell frequencies may impact efficacy. Specifically, HLA-I-restricted TCRs typically exhibit higher functional avidity in CD8+ T cells than in CD4+ T cells due to CD8-coreceptor-mediated enhancement of TCR engagement with HLA-I (52, 53). Consequently, infusion products skewed toward CD4+ T cells may

A

	Clinical-scale day 10 infusion products				
	Cell Count ($x10^9$)	Fold expansion (from D2)	% CD3	% CD8+ (of CD3)	% mTCRβ (of CD3)
CRI-5178 (A11-10mer TCR)	6.15	52.1	97.3	98.1	85.6
CRI-2890 (C08-9mer & C08-10mer TCR)	3.30	22.9	91.9	84.5	84.5

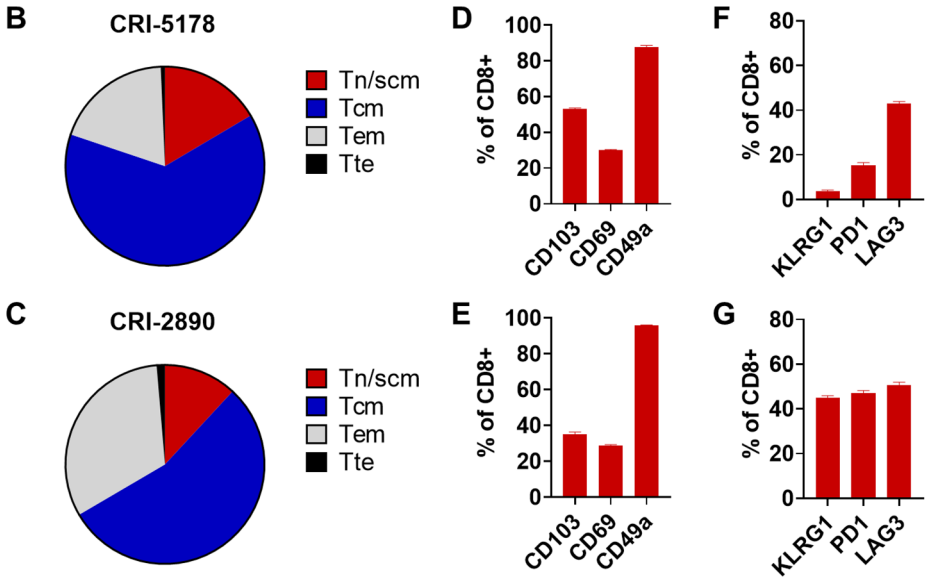

FIGURE 6
Cell number and phenotype of clinical-scale, 10-day CKT manufactured TCR-T cells. **(A)** Summary data for cell number (after LOVO harvest), fold expansion (from day 2 onwards), CD3 and CD8 frequencies, and transduction efficiency as determined by flow cytometric analysis of the mouse TCRβ constant region which is engineered into the TCRs. T-cell differentiation, tissue resident (Trm) and exhaustion/activation markers for TCR-T infusion products from CRI-5178 **(B, D, F)** and CRI-2890 **(C, E, G)** as determined by flow cytometric analysis. Tn/scm: CD45RO-CCR7+; Tcm: CD45RO+CCR7+; Tem: CD45RO+CCR7-; Tte: CD45RO-CCR7-.

exhibit suboptimal therapeutic activity. Indeed, this is supported by our preclinical work, where CD8-enriched TCR-T cells from two of three patient PBMC samples displayed improved tumor cell killing *in vitro* compared to bulk TCR-T cells (Supplementary Figure 5). Notably, recent TCR-T clinical trials targeting the tumor antigens MAGE-A4 (10) and PRAME (12) reported a median of ~ 50% CD4 + T cells in the final products, with some reaching as high as ~ 80%. To mitigate this inherent variability and ensure a defined and potentially more potent product, we incorporated a CD4+ cell depletion step to enrich CD8+ T cells during manufacturing. Another strategy to address this includes genetically engineering the bulk T-cell population to express CD8α (54) or CD8α/β co-receptors (52), an approach being explored in TCR-T clinical trials targeting MAGE-A4 (e.g., NCT04044859), PRAME (NCT03686124), and KRAS G12D (NCT06218914; biological product AZD0240).

Minimizing vein-to-vein time is critical for the clinical deployment of ex vivo cell therapies, particularly for patients with rapidly progressing disease. Manufacturing time for most TCR-T products typically ranges from seven days to a month, often with additional time for release testing, and thus our 10-day manufacturing process with fresh (non-cryopreserved) product infusion compares favorably. Infusion with fresh product is possible because our cleanroom facility is located at the hospital where patients would receive treatment. This point-of-care manufacturing model enables a shorter vein-to-vein time and mitigates the potential negative impacts of cryopreservation and thawing on the cell product.

Our study has several limitations. While our CKT-manufacturing process generated consistent trends on the phenotype and function of TCR-T cells across four patient samples, the biological diversity of patient-derived PBMCs will inevitably impact the final phenotype, yield, function, and ultimately, the antitumor potential of individual infusion products. Nonetheless, the use of patient-derived samples in this study represents an improvement over the healthy donor PBMCs commonly used in preclinical studies. When advancing an experimental cell therapy product toward larger-scale pivotal studies, a transition to simple, robust, automated, and closed systems is desirable. Our current 10-day manufacturing process involves significant manual manipulation, using tissue culture flasks during PBMC stimulation, columns for CD8 enrichment, and 6-well plates for transduction. Although this process is performed under GMP conditions and achieves therapeutic doses with high transduction efficiency in 10 days, further process development is

10.3389/fimmu.2026.1847411

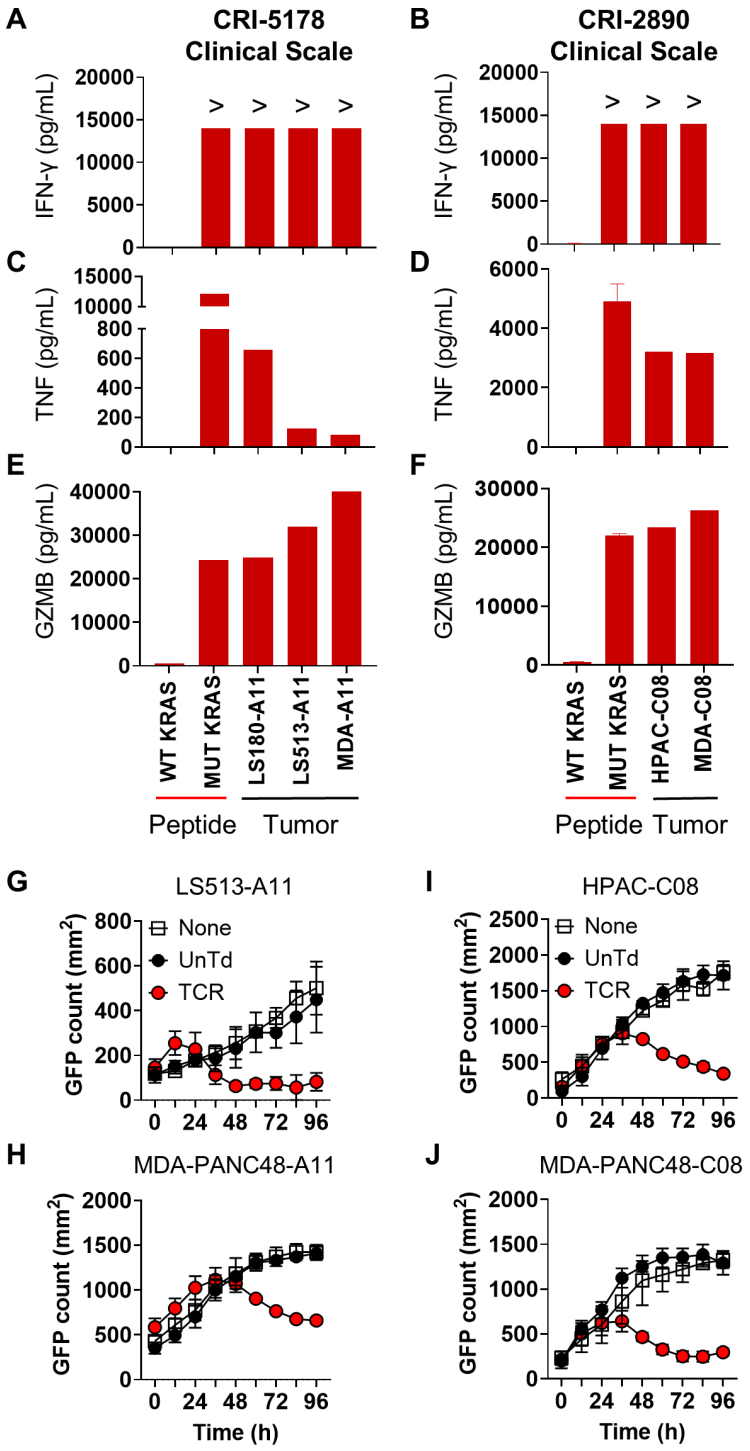

FIGURE 7
Effector function and antitumor activity of clinical-scale, 10-day CKT manufactured TCR-T cells. CRI-5178 10mer-A11 (left) or CRI-2890 9mer-C08 (right) TCR-T cells manufactured at clinical scale were cocultured overnight with the indicated KRAS G12D+ tumor cell lines expressing either HLA-A*11:01 (A11) or HLA-C*08:02 (C08) or autologous PBMC pulsed with 1 μg/mL of wild-type (WT) or mutated (MUT) KRAS peptide and **(A, B)** IFN-γ, **(C, D)** TNF, and **(E, F)** granzyme B (GZMB) was measured in the supernatants using the LegendPlex assay. **(G, H)** CRI-5178 10mer-A11 and **(I, J)** CRI-2890 9mer-C08 TCR-T were cocultured with the indicated KRAS G12D+ and A11 or C08 GFP-expressing tumor cell lines at an effector to target (E:T) ratio 1:2 in 2D culture and GFP was measured using the Cellcyte live cell imager. ">" greater than assay detection limit. None, tumor cells alone; UnTd, untransduced T cells. LEGENDplex data were from one experiment with technical replicates. Coculture assays are representative of at least 2 independent experiments.

required to implement automation in a closed system. The G-Rex technology used in this study supports closed-system processes, as do other platforms such as the CliniMACS Prodigy, which has been employed to develop TCR-T cells in an automated, closed, and GMP-compliant process (55, 56). Finally, our study is limited to *in vitro* characterization, and therefore it remains to be determined whether the desirable attributes imprinted by CKT on the TCR-T cells translate to improved control of tumors *in vivo*.

In conclusion, we have developed a 10-day, clinical-scale manufacturing protocol that utilizes a novel cytokine cocktail consisting of IL-2, IL-7, IL-15 and TGF-β to generate TCR-T cells with early memory and tissue-resident-like phenotypes and robust *in vitro* antitumor activity. We plan to evaluate the safety and efficacy of mutant KRAS-targeting TCR-T cells generated with this protocol in an upcoming clinical trial.

Data availability statement

The raw data supporting the conclusions of this article will be made available by the authors, without undue reservation.

Ethics statement

The studies involving humans were approved by the Institutional Review Board of Providence St. Joseph Health. The studies were conducted in accordance with the local legislation and institutional requirements. The participants provided their written informed consent to participate in this study.

Author contributions

YS: Conceptualization, Writing – review & editing, Methodology, Investigation, Writing – original draft, Visualization, Validation, Formal analysis. SD: Writing – original draft, Formal analysis, Visualization, Investigation, Writing – review & editing, Validation, Data curation. OB: Formal analysis, Data curation, Validation, Investigation, Writing – review & editing, Writing – original draft. HH: Data curation, Formal analysis, Validation, Investigation, Writing – review & editing. AL: Writing – review & editing, Investigation, Formal analysis, Data curation, Validation. MB: Investigation, Writing – review & editing, Formal analysis, Validation, Data curation. MJ: Writing – review & editing, Investigation, Validation, Formal analysis. MS: Writing – review & editing, Formal analysis, Validation, Investigation. LJ: Writing – review & editing, Investigation, Formal analysis. NS: Project administration, Supervision, Writing – review & editing. ET: Visualization, Resources, Validation, Formal analysis, Project administration, Conceptualization, Methodology, Writing – review & editing, Writing – original draft, Supervision, Funding acquisition.

Funding

The author(s) declared that financial support was received for this work and/or its publication. Providence Portland Medical Foundation (PPMF).

Acknowledgments

We thank the Providence Portland Medical Foundation (PPMF) and donors to the PPMF for funding this work. We also thank the G-Rex Grant Program for supporting this study. We are grateful to the patients and their families, and members of Providence Health and Services and the EACRI who were involved with patient care and sample acquisition.

Conflict of interest

ET is a consultant for Pathfinder Oncology and was a consultant for AstraZeneca and was on the scientific advisory board of Turnstone Biologics.

The remaining author(s) declared that this work was conducted in the absence of any commercial or financial relationships that could be construed as a potential conflict of interest.

Generative AI statement

The author(s) declared that generative AI was used in the creation of this manuscript. To provide alternative sentence structures and improve clarity in parts of the Discussion section. All AI outputs were manually reviewed and modified prior to incorporation into the manuscript.

Any alternative text (alt text) provided alongside figures in this article has been generated by Frontiers with the support of artificial intelligence and reasonable efforts have been made to ensure accuracy, including review by the authors wherever possible. If you identify any issues, please contact us.

Publisher's note

Supplementary material

The Supplementary Material for this article can be found online at: https://www.frontiersin.org/articles/10.3389/fimmu.2026.1847411/full#supplementary-material

References

1. D'Angelo SP, Druta M, Van Tine BA, Liebner D, Schuetze SM, Tap WD, et al. Letetresgene autoleucel in advanced/metastatic myxoid/round cell liposarcoma. *J Clin Oncol*. (2025) 43:1777–88. doi: 10.1200/JCO-24-01466

2. D'Angelo SP, Melchiori L, Merchant MS, Bernstein D, Glod J, Kaplan R, et al. Antitumor activity associated with prolonged persistence of adoptively transferred NY-ESO-1 (c259)T cells in synovial sarcoma. *Cancer Discov*. (2018) 8:944–57. doi: 10.1158/2159-8290.CD-17-1417

3. Kawai A, Ishihara M, Nakamura T, Kitano S, Iwata S, Takada K, et al. Safety and efficacy of NY-ESO-1 antigen-specific T-cell receptor gene-transduced T lymphocytes in patients with synovial sarcoma: a phase I/II clinical trial. *Clin Cancer Research: Off J Am Assoc For Cancer Res*. (2023) 29:5069–78. doi: 10.1158/1078-0432.ccr-23-1456

4. Ramachandran I, Lowther DE, Dryer-Minnerly R, Wang R, Fayngerts S, Nunez D, et al. Systemic and local immunity following adoptive transfer of NY-ESO-1 SPEAR T cells in synovial sarcoma. *J Immunother Cancer*. (2019) 7:276. doi: 10.1186/s40425-019-0762-2

5. Robbins PF, Kassim SH, Tran TL, Crystal JS, Morgan RA, Feldman SA, et al. A pilot trial using lymphocytes genetically engineered with an NY-ESO-1-reactive T-cell receptor: long-term follow-up and correlates with response. *Clin Cancer Research: Off J Am Assoc For Cancer Res*. (2015) 21:1019–27. doi: 10.1158/1078-0432.ccr-14-2708

6. Robbins PF, Morgan RA, Feldman SA, Yang JC, Sherry RM, Dudley ME, et al. Tumor regression in patients with metastatic synovial cell sarcoma and melanoma using genetically engineered lymphocytes reactive with NY-ESO-1. *J Clin Oncol*. (2011) 29:917–24. doi: 10.1200/jco.2010.32.2537

7. Pan Q, Weng D, Liu J, Han Z, Ou Y, Xu B, et al. Phase 1 clinical trial to assess safety and efficacy of NY-ESO-1-specific TCR T cells in HLA-A *02:01 patients with advanced soft tissue sarcoma. *Cell Rep Med*. (2023) 4:101133. doi: 10.1016/j.xcrm.2023.101133

8. Lu YC, Parker LL, Lu T, Zheng Z, Toomey MA, White DE, et al. Treatment of patients with metastatic cancer using a major histocompatibility complex class II-restricted T-cell receptor targeting the cancer germline antigen MAGE-A3. *J Clin Oncol*. (2017) 35:3322–9. doi: 10.1200/jco.2017.74.5463

9. Morgan RA, Chinnasamy N, Abate-Daga D, Gros A, Robbins PF, Zheng Z, et al. Cancer regression and neurological toxicity following anti-MAGE-A3 TCR gene therapy. *J Immunother*. (2013) 36:133–51. doi: 10.1097/cji.0b013e3182829903

10. D'Angelo SP, Araujo DM, Abdul Razak AR, Agulnik M, Attia S, Blay JY, et al. Afamitresgene autoleucel for advanced synovial sarcoma and myxoid round cell liposarcoma (SPEARHEAD-1): an international, open-label, phase 2 trial. *Lancet*. (2024) 403:1460–71. doi: 10.1891/9780826148537.0025

11. Hong DS, Van Tine BA, Biswas S, McAlpine C, Johnson ML, Olszanski AJ, et al. Autologous T cell therapy for MAGE-A4(+) solid cancers in HLA-A*02(+) patients: a phase 1 trial. *Nat Med*. (2023) 29:104–14. doi: 10.1038/s41591-022-02128-z

12. Wermke M, Araujo DM, Chatterjee M, Tsimberidou AM, Holderried TAW, Jazaeri AA, et al. Autologous T cell therapy for PRAME(+) advanced solid tumors in HLA-A*02 (+) patients: a phase 1 trial. *Nat Med*. (2025) 31:2365–74. doi: 10.1038/s41591-025-03650-6

13. Doran SL, Stevanovic S, Adhikary S, Gartner JJ, Jia L, Kwong MLM, et al. T-cell receptor gene therapy for human papillomavirus-associated epithelial cancers: a first-in-human, phase I/II study. *J Clin Oncol*. (2019) 37:2759–68. doi: 10.1200/jco.18.02424

14. Nagarsheth NB, Norberg SM, Sinkoe AL, Adhikary S, Meyer TJ, Lack JB, et al. TCR-engineered T cells targeting E7 for patients with metastatic HPV-associated epithelial cancers. *Nat Med*. (2021) 27:419–25. doi: 10.1038/s41591-020-01225-1

15. Kim SP, Vale NR, Zacharakis N, Krishna S, Yu Z, Gasmi B, et al. Adoptive cellular therapy with autologous tumor-infiltrating lymphocytes and T-cell receptor-engineered T cells targeting common p53 neoantigens in human solid tumors. *Cancer Immunol Res*. (2022) 10:932–46. doi: 10.1158/2326-6066.cir-22-0040

16. Leidner R, Sanjuan Silva N, Huang H, Sprott D, Zheng C, Shih YP, et al. Neoantigen T-cell receptor gene therapy in pancreatic cancer. *N Engl J Med*. (2022) 386:2112–19. doi: 10.1056/nejmoa2119662

17. Parkhurst M, Goff SL, Lowery FJ, Beyer RK, Halas H, Robbins PF, et al. Adoptive transfer of personalized neoantigen-reactive TCR-transduced T cells in metastatic colorectal cancer: phase 2 trial interim results. *Nat Med*. (2024) 30:2586–95. doi: 10.1038/s41591-024-03109-0

18. Gattinoni L, Speiser DE, Lichterfeld M, Bonini C. T memory stem cells in health and disease. *Nat Med*. (2017) 23:18–27. doi: 10.1038/nm.4241

19. Krishna S, Lowery FJ, Copeland AR, Bahadiroglu E, Mukherjee R, Jia L, et al. Stem-like CD8 T cells mediate response of adoptive cell immunotherapy against human cancer. *Science*. (2020) 370:1328–34. doi: 10.1126/science.abb9847

20. Filosto S, Vardhanabhuti S, Canales MA, Poire X, Lekakis LJ, de Vos S, et al. Product attributes of CAR T-cell therapy differentially associate with efficacy and toxicity in second-line large B-cell lymphoma (ZUMA-7). *Blood Cancer Discov*. (2024) 5:21–33. doi: 10.1158/2643-3230.bcd-23-0112

21. Deng Q, Han G, Puebla-Osorio N, Ma MCJ, Strati P, Chasen B, et al. Characteristics of anti-CD19 CAR T cell infusion products associated with efficacy and toxicity in patients with large B cell lymphomas. *Nat Med*. (2020) 26:1878–87. doi: 10.1038/s41591-020-1061-7

22. Bai Z, Woodhouse S, Zhao Z, Arya R, Govek K, Kim D, et al. Single-cell antigen-specific landscape of CAR T infusion product identifies determinants of CD19-positive relapse in patients with ALL. *Sci Adv*. (2022) 8:eabj2820. doi: 10.1126/sciadv.abj2820

23. Haradhvala NJ, Leick MB, Maurer K, Gohil SH, Larson RC, Yao N, et al. Distinct cellular dynamics associated with response to CAR-T therapy for refractory B cell lymphoma. *Nat Med*. (2022) 28:1848–59. doi: 10.1038/s41591-022-01959-0

24. Biasco L, Izotova N, Rivat C, Ghorashian S, Richardson R, Guvenel A, et al. Clonal expansion of T memory stem cells determines early anti-leukemic responses and long-term CAR T cell persistence in patients. *Nat Cancer*. (2021) 2:629–42. doi: 10.1038/s43018-021-00207-7

25. Gavil NV, Cheng K, Masopust D. Resident memory T cells and cancer. *Immunity*. (2024) 57:1734–51. doi: 10.1016/j.immuni.2024.06.017

26. Ramirez DE, Mohamed A, Huang YH, Turk MJ. In the right place at the right time: tissue-resident memory T cells in immunity to cancer. *Curr Opin Immunol*. (2023) 83:102338. doi: 10.1016/j.coi.2023.102338

27. Jung IY, Noguera-Ortega E, Bartoszek R, Collins SM, Williams E, Davis M, et al. Tissue-resident memory CAR T cells with stem-like characteristics display enhanced efficacy against solid and liquid tumors. *Cell Rep Med*. (2023) 4:101053. doi: 10.1016/j.xcrm.2023.101053

28. Liikanen I, Lauhan C, Quon S, Omilusik K, Phan AT, Bartroli LB, et al. Hypoxia-inducible factor activity promotes antitumor effector function and tissue residency by CD8+ T cells. *J Clin Invest*. (2021) 131(7):e143729. doi: 10.1172/jci143729

29. Milner JJ, Toma C, Yu B, Zhang K, Omilusik K, Phan AT, et al. Runx3 programs CD8(+) T cell residency in non-lymphoid tissues and tumours. *Nature*. (2017) 552:253–7. doi: 10.1038/nature24993

30. Alizadeh D, Wong RA, Yang X, Wang D, Pecoraro JR, Kuo CF, et al. IL15 enhances CAR-T cell antitumor activity by reducing mTORC1 activity and preserving their stem cell memory phenotype. *Cancer Immunol Res*. (2019) 7:759–72. doi: 10.1158/2326-6066.cir-18-0466

31. Alvarez-Fernandez C, Escriba-Garcia L, Vidal S, Sierra J, Briones J. A short CD3/CD28 costimulation combined with IL-21 enhance the generation of human memory stem T cells for adoptive immunotherapy. *J Transl Med*. (2016) 14:214. doi: 10.1182/blood.v126.23.5424.5424

32. Cieri N, Camisa B, Cocchiarella F, Forcato M, Oliveira G, Provasi E, et al. IL-7 and IL-15 instruct the generation of human memory stem T cells from naive precursors. *Blood*. (2013) 121:573–84. doi: 10.1182/blood-2012-05-431718

33. Gomez-Eerland R, Nuijen B, Heemskerk B, van Rooij N, van den Berg JH, Beijnen JH, et al. Manufacture of gene-modified human T-cells with a memory stem/central memory phenotype. *Hum Gene Ther Methods*. (2014) 25:277–87. doi: 10.1089/hgtb.2014.004

34. Lamers CH, van Steenbergen-Langeveld S, van Brakel M, Groot-van Ruijven CM, van Elzakker PM, van Krimpen B, et al. T cell receptor-engineered T cells to treat solid tumors: T cell processing toward optimal T cell fitness. *Hum Gene Ther Methods*. (2014) 25:345–57. doi: 10.1089/hgtb.2014.051

35. Levin N, Paria BC, Vale NR, Yossef R, Lowery FJ, Parkhurst MR, et al. Identification and validation of T-cell receptors targeting RAS hotspot mutations in human cancers for use in cell-based immunotherapy. *Clin Cancer Research: Off J Am Assoc For Cancer Res*. (2021) 27:5084–95. doi: 10.1158/1078-0432.ccr-21-0849

36. Tran E, Robbins PF, Lu YC, Prickett TD, Gartner JJ, Jia L, et al. T-cell transfer therapy targeting mutant KRAS in cancer. *N Engl J Med*. (2016) 375:2255–62. doi: 10.1056/nejmoa1609279

37. Kalia V, Sarkar S, Subramaniam S, Haining WN, Smith KA, Ahmed R. Prolonged interleukin-2Ralpha expression on virus-specific CD8+ T cells favors terminal-effector differentiation *in vivo*. *Immunity*. (2010) 32:91–103. doi: 10.1016/j.immuni.2009.11.010

38. Pipkin ME, Sacks JA, Cruz-Guilloty F, Lichtenheld MG, Bevan MJ, Rao A. Interleukin-2 and inflammation induce distinct transcriptional programs that promote the differentiation of effector cytolytic T cells. *Immunity*. (2010) 32:79–90. doi: 10.1016/j.immuni.2009.11.012

39. Nixon BG, Gao S, Wang X, Li MO. TGFbeta control of immune responses in cancer: a holistic immuno-oncology perspective. *Nat Rev Immunol*. (2023) 23:346–62. doi: 10.1038/s41577-022-00796-z

40. Casey KA, Fraser KA, Schenkel JM, Moran A, Abt MC, Beura LK, et al. Antigen-independent differentiation and maintenance of effector-like resident memory T cells in tissues. *J Immunol*. (2012) 188:4866–75. doi: 10.4049/jimmunol.1200402

41. El-Asady R, Yuan R, Liu K, Wang D, Gress RE, Lucas PJ, et al. TGF-beta-dependent CD103 expression by CD8(+) T cells promotes selective destruction of the host intestinal epithelium during graft-versus-host disease. *J Exp Med*. (2005) 201:1647–57. doi: 10.1007/978-3-540-29676-8_729

42. Kilshaw PJ, Murant SJ. Expression and regulation of beta 7(beta p) integrins on mouse lymphocytes: relevance to the mucosal immune system. *Eur J Immunol*. (1991) 21:2591–7. doi: 10.1002/eji.1830211041

43. Mackay LK, Rahimpour A, Ma JZ, Collins N, Stock AT, Hafon ML, et al. The developmental pathway for CD103(+)CD8+ tissue-resident memory T cells of skin. *Nat Immunol*. (2013) 14:1294–303. doi: 10.1038/ni.2744

44. Zhang N, Bevan MJ. Transforming growth factor-beta signaling controls the formation and maintenance of gut-resident memory T cells by regulating migration and retention. *Immunity*. (2013) 39:687–96. doi: 10.1016/j.immuni.2013.08.019

45. Liu S, Etto T, Rodriguez-Cruz T, Li Y, Wu C, Fulbright OJ, et al. TGF-beta1 induces preferential rapid expansion and persistence of tumor antigen-specific CD8+ T cells for adoptive immunotherapy. *J Immunother*. (2010) 33:371–81. doi: 10.1097/cji.0b013e3181cd1180

46. Dahmani A, Janelle V, Carli C, Richaud M, Lamarche C, Khalili M, et al. TGFbeta programs central memory differentiation in ex vivo-stimulated human T cells. *Cancer Immunol Res*. (2019) 7:1426–39. doi: 10.1158/2326-6066.cir-18-0691

47. Schober SL, Kuo CT, Schluns KS, Lefrancois L, Leiden JM, Jameson SC. Expression of the transcription factor lung Kruppel-like factor is regulated by cytokines and correlates with survival of memory T cells *in vitro* and *in vivo*. *J Immunol*. (1999) 163:3662–7. doi: 10.4049/jimmunol.163.7.3662

48. Sinclair LV, Finlay D, Feijoo C, Cornish GH, Gray A, Ager A, et al. Phosphatidylinositol-3-OH kinase and nutrient-sensing mTOR pathways control T lymphocyte trafficking. *Nat Immunol*. (2008) 9:513–21. doi: 10.1038/ni.1603

49. Beatson RE, Parente-Pereira AC, Halim L, Cozzetto D, Hull C, Whilding LM, et al. TGF-beta1 potentiates Vgamma9Vdelta2 T cell adoptive immunotherapy of cancer. *Cell Rep Med*. (2021) 2:100473. doi: 10.1016/j.xcrm.2021.100473

50. Peters C, Meyer A, Kouakanou L, Feder J, Schricker T, Lettau M, et al. TGF-beta enhances the cytotoxic activity of Vdelta2 T cells. *Oncoimmunology*. (2019) 8:e1522471. doi: 10.1080/2162402x.2018.1522471

51. Foy SP, Jacoby K, Bota DA, Hunter T, Pan Z, Stawiski E, et al. Non-viral precision T cell receptor replacement for personalized cell therapy. *Nature*. (2023) 615:687–96. doi: 10.1038/s41586-022-05531-1

52. Xue SA, Gao L, Ahmadi M, Ghorashian S, Barros RD, Pospori C, et al. Human MHC Class I-restricted high avidity CD4(+) T cells generated by co-transfer of TCR and CD8 mediate efficient tumor rejection *in vivo*. *Oncoimmunology*. (2013) 2:e22590. doi: 10.4161/onci.22590

53. Kessels HW, Schepers K, van den Boom MD, Topham DJ, Schumacher TN. Generation of T cell help through a MHC class I-restricted TCR. *J Immunol*. (2006) 177:976–82. doi: 10.4049/jimmunol.177.2.976

54. Anderson VE, Brilha SS, Weber AM, Pachnio A, Wiedermann GE, Dauleh S, et al. Enhancing efficacy of TCR-engineered CD4 + T cells via coexpression of CD8alpha. *J Immunother*. (2023) 46:132–44. doi: 10.1097/cji.0000000000000456

55. Yonezawa Ogusuku IE, Herbel V, Lennartz S, Brandes C, Argiro E, Fabian C, et al. Automated manufacture of DeltaNPM1 TCR-engineered T cells for AML therapy. *Mol Ther Methods Clin Dev*. (2024) 32:101224. doi: 10.1016/j.omtm.2024.101224

56. Silva DN, Chrobok M, Rovesti G, Healy K, Wagner AK, Maravelia P, et al. Process development for adoptive cell therapy in academia: A pipeline for clinical-scale manufacturing of multiple TCR-T cell products. *Front Immunol*. (2022) 13:896242. doi: 10.3389/fimmu.2022.896242